Available online at www.sciencedirect.com
SCIENCE DIRECT
Journal of Colloid and Interface Science 281 (2005) 495–502
JOURNAL OF Colloid and Interface Science
www.elsevier.com/locate/jcis

Entropic interfaces in hard-core model amphiphilic mixtures

Joseph M. Brader [a,*], Matthias Schmidt [b,1]

[a] *Institute of Physiology, University of Bern, Bühlplatz 5, 3012 Bern, Switzerland*
[b] *Soft Condensed Matter Group, Debye Institute, Utrecht University, Princetonpln 5, 3584 CC Utrecht, The Netherlands*

Received 11 June 2004; accepted 11 August 2004
Available online 27 October 2004

Abstract

We investigate bulk and interfacial properties of a recently proposed hard-body model for a ternary mixture of amphiphilic particles, spheres and needles using density functional theory. The simple model amphiphiles are formed by bonding a vanishingly thin needle tail radially to a hard-sphere head group. Such particles provide a natural amphiphile when added to a binary mixture of spheres and needles. As all interactions are hard, we seek to find whether amphiphilic effects can be driven by entropy without the need to invoke attractive interactions. In order to assess the amphiphilic character of the model we first examine the spatial and orientational distribution of the amphiphiles at the free interface between demixed needle-rich and amphiphile-rich fluid phases of the binary amphiphile–needle subsystem. We then consider the free interface between sphere-rich and needle-rich phases upon adding amphiphiles with low concentration to the demixed system. In both cases the orientational distribution of the particles in the interface provides strong evidence that amphiphilic properties can arise purely from geometrical packing effects.

1. Introduction

Amphiphilic molecules are characterized by a hydrophilic head group and a hydrophobic tail. The preferential adsorption of amphiphiles at oil–water interfaces facilitates phase separation and thus gives rise to numerous industrial and domestic applications. It is generally accepted that attractive interactions play a large role in both driving and stabilizing amphiphilic order. The coupling between attractive forces and the intrinsic particle geometry produces the spatial and orientational distributions characteristic of amphiphilic systems. However, it is not clear whether attractive interactions are a fundamental requirement to reproduce the phenomenology of amphiphilic systems, or whether attraction simply provides a stabilizing mechanism for an essentially entropic phenomenon. In this paper we seek to clarify this point by investigating the properties of a model entropic amphiphile system in the presence of inhomogeneity. Our study is not only of interest from a pure statistical mechanics point of view; with the increasing experimental accessibility of colloidal systems, in which energetic effects can be largely suppressed, come realistic possibilities for the study of hard-body amphiphiles. Significant advances have been made in the fabrication of colloidal particles with more complex geometry by the adhesion of simpler colloidal particles. A report of experimental progress in the study of such "colloidal molecules" can be found in [1] in which the authors construct composite particles by bonding spheres together into doublet, triplet, and tetrahedral clusters.

We pose the simple question: Can amphiphilic effects arise solely from the geometrical properties of the particles? That entropy could drive amphiphilic behavior does not seem unreasonable; many of the phenomena usually associated with attractive interactions, such as phase separation [2–5] or wetting at substrates [6–11], have been observed in entropic systems. It is well established that simple

* Corresponding author. Fax: +41-31-631-46-11.
E-mail address: brader@cns.unibe.ch (J.M. Brader).
[1] On leave from: Institut für Theoretische Physik II, Heinrich-Heine-Universität Düsseldorf, Universitätsstraße 1, D-40225 Düsseldorf, Germany.

0021-9797/$ – see front matter
doi:10.1016/j.jcis.2004.08.097

hard spheres provide a good model of certain suspensions of spherical colloids; however, hard-particle models can also be useful in accounting for the behavior of considerably more complex soft-matter systems. One of the early examples of this approach originated in the 1954 paper of Asakura and Oosawa, where they proposed a mechanism by which an effective attraction could arise between two large spherical colloidal particles immersed in a sea of rigid, but mutually interpenetrable, macromolecules, the now familiar "depletion attraction" [12]. In a subsequent work Asakura and Oosawa considered the depletion attraction as a possible mechanism for the aggregation of colloids in colloid–polymer mixtures [13]. In 1976 Vrij independently proposed the same mechanism for aggregation and defined an explicit model Hamiltonian for a colloid–polymer mixture, now termed the Asakura–Oosawa–Vrij or simply the AO model [14]. This model is a binary hard-sphere mixture in which the mutual interaction between molecules of one of the species is set equal to zero in order to mimic the behavior of spherical polymer coils at low concentration or theta point conditions. Despite the simplicity of the interactions this model provides a reasonable description of the bulk fluid–fluid phase separation observed in real colloid–polymer mixtures [3–5,15,16] and predicts a rich variety of inhomogeneous phenomena [6, 17,18], some of which have been observed in experiments [7–10] and in simulations [19]. In a similar spirit, Bolhuis and Frenkel (BF) proposed a model for a binary mixture of spheres and rodlike particles [20] which played an important role in motivating a number of subsequent experimental studies [2,21–23]. The spherical colloids are again modeled as hard spheres and the rodlike particles are taken to be infinitely thin needles of a given length. The bulk phase behavior predicted by this model is found to agree favorably with that of real colloidal rod–sphere mixtures [2,24]. Due to the simple nature of the interparticle interactions, accurate approximate theories have been constructed for both the AO and BF rod–sphere models. A good description of the bulk-phase equilibria is given by free-volume theory [20,24, 25] whereas inhomogeneous situations can be successfully treated using modern developments in density functional theory [26–28].

As a simple model for an amphiphilic system Bolhuis and Frenkel considered amphiphilic particles constructed by bonding a hard-sphere "head group" to a spherocylinder "tail" [29]. The tails are taken to be mutually noninteracting but retain a hard repulsion with respect to the head group. The behavior of these model particles was found to mimic that of real amphiphiles when they are immersed in a sea of hard spheres. The most recent model in this hierarchy, and the subject of the present study, is a generalization of the sphere–needle model to a ternary mixture of amphiphiles, spheres and needles [30], in which amphiphile particles are constructed by radially bonding a needle to a sphere surface. The use of needles rather than spherocylinders makes the model amenable to theoretical analysis which is, at present, not possible for the BF model amphiphiles. For a recent review of hard-particle models we refer the reader to [31]. Despite the simplicity of our model amphiphiles an experimental realization still presents a considerable challenge. Spherical PMMA, polystyrene, or silica particles all provide a good approximation to idealized hard spheres and thin boehmite rods coated with silica have properties similar to our ideal needles. Fusion of these existing particles would well approximate our amphiphilic particles.

In this paper we investigate the distribution of hard-body amphiphilic particles at the interface between two fluid phases. We both extend and draw connections between previous studies in which the free interface between demixed fluid phases in the binary needle–sphere mixture [32] and the adsorption at a hard wall of the same model amphiphiles [33] were considered. In order to fully assess the ternary mixture we have followed a systematic program consisting of a full investigation of the bulk thermodynamics of the three binary subsystems [30], namely the sphere–needle (SN), amphiphile–needle (AN), and amphiphile–sphere (AS) mixtures, a study of the pure amphiphilic system adsorbed at a hard wall [33] and of the free interface in the demixed SN system [32]. Here we extend the study of [32] and investigate the free interface of the AN mixture. We then consider the full ternary amphiphile–sphere–needle (ASN) mixture and analyze the distribution of amphiphiles in the free interface between demixed sphere-rich and needle-rich phases when small concentrations of amphiphile are added.

The paper is organized as follows. In Section 2 we define the model. In Section 3 we give a description of the density functional theory and define the order parameters used for quantitative analysis. In Section 4 we present our results and in Section 5 we give concluding remarks and present possibilities for future study.

2. The model

We consider a ternary mixture consisting of amphiphiles, needles, and spheres [30]. Fig. 1 shows a sketch of the mixture. The interaction between particles is infinitely repulsive

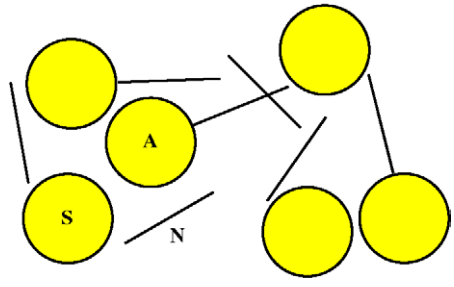

Fig. 1. The model ternary mixture consisting of amphiphiles (A), spheres (S), and needles (N). All interactions are infinitely repulsive for spatial overlaps. The needles are of vanishing thickness and, therefore, have no mutual interaction. The amphiphile particles are formed by bonding a needle radially to a sphere surface.

for spatially overlapping configurations and zero otherwise. The amphiphilic particles consist of a hard sphere of diameter σ_A and an infinitely thin needle of length L_A bonded radially to the sphere surface. We will henceforth refer to the sphere as the amphiphile "head" and the bonded needle as the "tail." The position vector $\mathbf{r}$ which locates the particle is taken to be the center point of the sphere and the direction of the tail is specified by a unit vector $\boldsymbol{\Omega}$ which, in the planar geometry under consideration, lies at an angle of θ to the z-axis. When calculating inhomogeneous density profiles we choose a coordinate system such that $\theta = 0$ corresponds to a particle configuration where the tail points in the negative z-direction. The needles have length L_N and, as they are of vanishing thickness, have no mutual interaction. The third species are simple hard spheres of diameter σ_S. In order to reduce the number of free parameters we consider the special case $\sigma \equiv \sigma_A = \sigma_S$, $L \equiv L_A = L_S$, and $\sigma = L$. With the size ratios thus specified we are left with three thermodynamic control parameters, $\eta_S \equiv \sigma_S^3 \pi \rho_S/6$, the packing fraction of spheres, $\eta_A \equiv \sigma_A^3 \pi \rho_A/6$, the packing fraction of the spherical amphiphile heads and the reduced needle density $\rho_* \equiv \sigma_N L_N^2 \rho_N$. It is to be emphasized that the theory is in no way constrained by our choice of size ratios and calculations for other choices of σ_S, σ_A, L_S, and L_A are no more difficult than for the case we study here.

The model we employ is closely related to that of Bolhuis and Frenkel [29]; in fact the BF model amphiphile is obtained by simply replacing the needle tail with a mutually noninteracting spherocylinder. The two models become identical in the limit of vanishing spherocylinder radius. For nonzero spherocylinder radii the present model is much more accessible to theoretical analysis than the BF model. From a conceptual point of view our model is rather different from that of BF, as it is fully additive; the noninteracting nature of the tails arises as a consequence of the vanishing thickness. Needle interactions can then be included, if necessary, to second virial level in the spirit of Onsager [34], albeit at the expense of increased computational complexity [35].

3. Method

Density functional theory (DFT) is a powerful tool in the study of inhomogeneous fluids [36]. We employ the DFT of [30], which successfully extends Rosenfeld's fundamental measures theory [37,38] to systems of nonconvex particles with orientational degrees of freedom. Although we consider only the special case of a ternary mixture, the theory is formulated for a general multicomponent mixture of spheres, needles, and amphiphiles, with arbitrary size ratios between species. Within the framework of fundamental measure theory the excess free energy is expressed as the spatial integral over a function of weighted densities. The weighted densities are constructed by convolving the equilibrium density profile with geometrically determined weight functions which are characteristic of the particle shapes. For details we refer the reader to [30]. Numerical minimization of the functional for inhomogeneous situations is performed using standard iterative techniques [32]. In the case of the ternary ASN mixture we have to minimize the grand potential, Ω, with respect to variation of three inhomogeneous density profiles, $\delta\Omega/\delta\rho_A(\mathbf{r}, \boldsymbol{\Omega}) = \delta\Omega/\delta\rho_N(\mathbf{r}, \boldsymbol{\Omega}) = \delta\Omega/\delta\rho_S(\mathbf{r}) = 0$, where $\rho_A(\mathbf{r}, \boldsymbol{\Omega})$, $\rho_N(\mathbf{r}, \boldsymbol{\Omega})$, and $\rho_S(\mathbf{r})$ are the density profiles of amphiphiles, needles, and spheres, respectively. To obtain free interface profiles is somewhat easier than in the case of a discontinuous external potential [33], where the complex nonconvex shape of the model amphiphiles demands a very careful treatment of the angular discretization.

In order to analyze the behavior of the nonspherical particles we consider two characteristic distributions obtained from the full profiles $\rho_i(\mathbf{r}, \boldsymbol{\Omega})$, $i = A, N$. The first is the orientation-averaged profile which describes the distribution of the centers of mass,

$$\bar{\rho}_i(\mathbf{r}) = \int \frac{d^2\Omega}{4\pi} \rho_i(\mathbf{r}, \boldsymbol{\Omega}). \tag{1}$$

The second is an orientational order parameter, which is different for needles and amphiphiles. For amphiphiles we consider the average

$$\langle \cos\theta \rangle = \bar{\rho}_A(\mathbf{r})^{-1} \int \frac{d^2\Omega}{4\pi} \rho_A(\mathbf{r}, \boldsymbol{\Omega}) \cos\theta, \tag{2}$$

whereas for the needles, due to the inflection symmetry $\boldsymbol{\Omega} \to -\boldsymbol{\Omega}$, we use

$$\langle P_2(\cos\theta) \rangle = \bar{\rho}_N(\mathbf{r})^{-1} \int \frac{d^2\Omega}{4\pi} \rho_N(\mathbf{r}, \boldsymbol{\Omega}) P_2(\cos\theta), \tag{3}$$

where $P_2(x) = (3x^2 - 1)/2$ is the second Legendre polynomial. For free interface studies of the ternary mixture we set the coordinate origin (in z) to the position of the Gibbs dividing surface for spheres; i.e., $\int_{-\infty}^{0} dz\, (\rho_s(z) - \rho_s(-\infty)) + \int_{0}^{\infty} dz\, (\rho_s(z) - \rho_s(\infty)) = 0$. For the AN mixture we fix the origin according to the Gibbs dividing surface of amphiphiles.

4. Results

4.1. Amphiphile–needle binary mixture

The AN mixture is similar to the SN mixture, with the important distinction that both species possess orientational order. The angular distribution of amphiphiles in the interface between demixed phases constitutes the first true test of the amphiphilic character of the model, beyond the initial indications provided by trends in the bulk phase equilibria [30] and the structure of the one-component amphiphile system adsorbed at a hard-wall substrate [33]. Due to the similarity of the AN and SN binary mixtures we expect there to be a close correspondence between $\rho_S(\mathbf{r})$ in the SN mixture and $\bar{\rho}_A(\mathbf{r})$ in the AN mixture. Indeed, the noninteracting character of the amphiphile tails suggests that for fluid states it

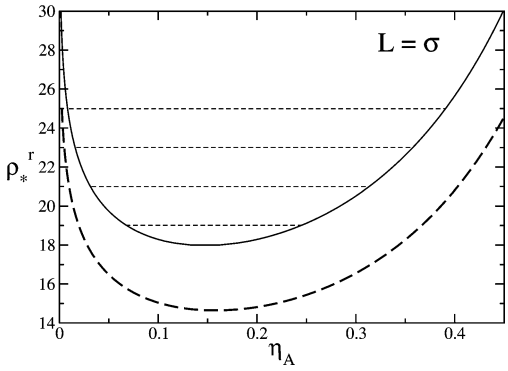

Fig. 2. The bulk fluid–fluid demixing phase diagram of the AN mixture for $L = \sigma$, where L is the tail length and σ is the sphere diameter, as a function of amphiphile packing fraction η_A and scaled needle reservoir density, ρ_*^r. The tie lines correspond to $\rho_*^r = 19, 21, 23, 25$ (from bottom to top) and indicate the coexisting states for which we perform detailed studies of the free interface. The broken line shows the phase boundary of the SN mixture for comparison, where the horizontal axis denotes the packing fraction of spheres, η_S.

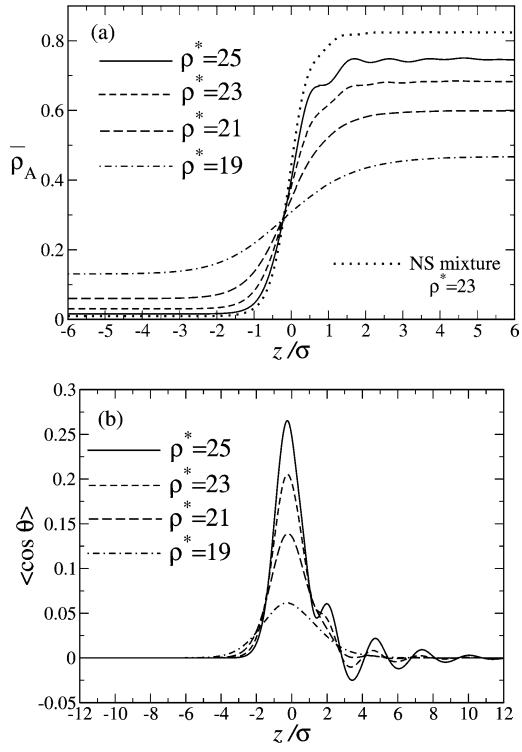

Fig. 3. The angle-averaged density profile of amphiphiles, $\bar{\rho}_A(z)$, as a function of the scaled coordinate perpendicular to the interface, z/σ, in the AN binary mixture. Results are shown for needle reservoir density $\rho_*^r = 19, 21, 23, 25$ corresponding to the state points marked in Fig. 2. The sphere profile of the SN mixture at $\rho_*^r = 23$ is also shown for comparison. Although the coexisting sphere liquid is denser than in the corresponding AN mixture, the oscillations are less pronounced. (b) The orientational order parameter for amphiphiles, $\langle \cos\theta \rangle$, as a function of z/σ in the AN binary mixture. The positive peak demonstrates the tendency for the amphiphile tails to point into the needle-rich phase.

may be useful to regard the AN mixture as a perturbed SN mixture.

For simplicity we consider the case $L_A = L_N = \sigma_A$. It is convenient to present results in a semi-grand-canonical ensemble in which the amphiphiles are treated canonically but are coupled to a reservoir of needles at fixed chemical potential. Fig. 2 shows the bulk fluid–fluid binodal in this (η_A, ρ_*^r) plane, where $\rho_*^r = \sigma_N L_N^2 \rho_N^r$ is the reduced needle density in the reservoir. For the present size ratio, the critical point of the AN mixture lies at larger values of ρ_*^r than for the equivalent SN mixture with $L_N = \sigma_S$. This is an intuitive result, as the replacement of spheres by amphiphiles suppresses the tendency to demix. The presence of the amphiphile tails increases the similarity of the two species in the mixture and thus enhances their miscibility.

We now consider the properties of the planar interface between demixed needle-rich and amphiphile-rich fluid phases. The four tie-lines in Fig. 2 are located at $\rho_*^r = 19$, 21, 23, and 25 and indicate the states for which we carry out detailed structural investigation of the interface. In this (η_A, ρ_*^r) representation the tie lines are horizontal, which is simply a consequence of coupling the system to a needle reservoir. The tie lines become skewed in a fully canonical (η_A, ρ_*) representation.

The profiles in Fig. 3a show the angle-averaged density of amphiphiles through the interface. As anticipated, the profiles closely resemble those of the spheres in the SN mixture when calculated at equivalent state points. However, the oscillations which occur on the amphiphile-rich side of the interface for larger values of ρ_*^r have larger amplitude than those seen in the sphere profiles of the SN mixture [35]. Comparison between the binodal curves for the present AN mixture and the SN mixture shows that, for a given ρ_*^r value, the coexisting sphere liquid density is considerably larger for the SN mixture than the corresponding amphiphile liquid density in the AN mixture. We can therefore conclude that the enhanced oscillations present in the $\bar{\rho}_A(\mathbf{r})$ profile are not due to simple differences in the bulk phase boundary. Larger differences between coexisting gas and liquid densities give rise to a sharper interface and therefore increase packing effects. The fact that the difference in coexisting densities is smaller in the AN mixture, for a given ρ_*^r value, than for the SN mixture, suggests that the presence of the tails enhances the packing structure of amphiphiles over that of pure spheres. Indeed, examination of the hard-wall profiles in [33] gave preliminary evidence that at liquid densities the amphiphile profiles tend to be more structured than their sphere counterparts. As the crystalline phases of the mixture are not known, the largest needle reservoir packing we consider is $\rho_*^r = 25$, for which the coexisting amphiphile liquid lies at $\eta_A \sim 0.4$. Provided the region of fluid–solid coexistence for the AN mixture is not substantially different from that of the SN mixture the state points considered here should all remain safely below the triple point.

Fig. 3b shows the orientational order parameter for amphiphiles, a value of $+1$ (-1) corresponds to total perpendicular (parallel) alignment of the amphiphile tails with respect to the interface. The state point $\rho_*^r = 19$ lies close to

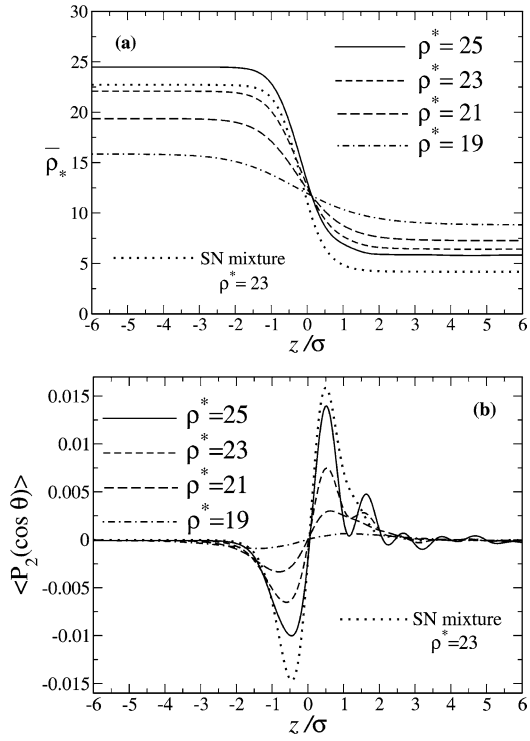

Fig. 4. The needle order parameters in the AN mixture as a function of the scaled coordinate perpendicular to the interface, z/σ. (a) The angle-averaged needle density, $\bar{\rho}_*$. (b) The orientational order parameter, $\langle P_2(\cos\theta)\rangle$. In both cases we display the needle order parameters for the SN mixture at $\rho_*^r = 23$ for comparison. Although the magnitude of the orientational ordering is clearly larger in the SN mixture, due to differences in the bulk phase diagram, the needles exhibit considerably more structure.

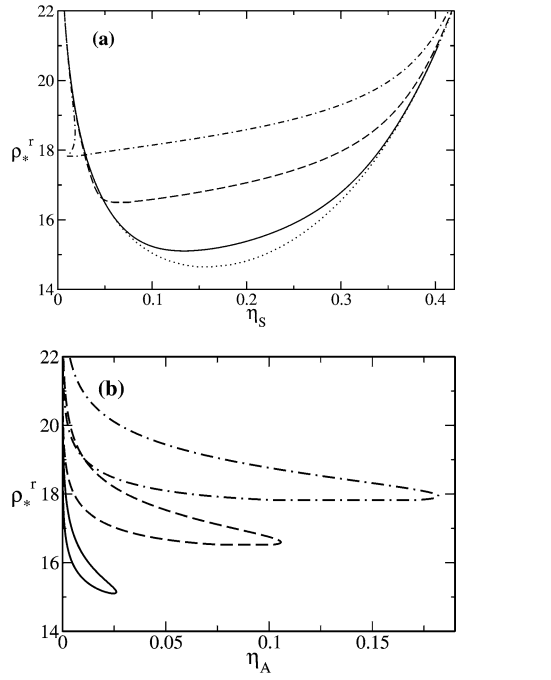

Fig. 5. The bulk phase diagram of the ternary ASN mixture. (a) The (η_S, ρ_*^r) plane for a fixed amphiphile chemical potential μ_A. Dotted line, $\mu_A = 0$, solid line, $\mu_A = 15$, broken line, $\mu_A = 18$, and dot-dashed line, $\mu_A = 20$. (b) The (η_A, ρ_*^r) plane for $\mu_A = 15$, 18, and 20. In both representations the tie lines are horizontal.

the bulk critical point and the interface is diffuse with correspondingly weak orientational order, the maximum value of $\langle\cos\theta\rangle$ only reaching $\sim$0.05. Nevertheless, the amphiphile tails still display a clear tendency to point into the needle-rich phase, even though the spatial density variation is weak. For larger values of ρ_*^r the effect increases significantly. For $\rho_*^r = 25$, the highest value considered, the peak in the distribution reaches $\sim$0.25, indicating strong orientational ordering at the interface. These orientational distributions provide the first indication that our hard body particles can behave as realistic amphiphiles in the presence of inhomogeneity. On the amphiphile-rich side of the interface $\langle\cos\theta\rangle$ shows oscillatory behavior (Fig. 3b), similar to the oscillations in $\bar{\rho}_A$ (Fig. 3a). This suggests a strong coupling between center-of-mass and orientational order.

The needle order parameters, shown in Figs. 4a and 4b, lend further evidence for increased spatial–orientational coupling in the AN mixture relative to the SN mixture. For a given value of ρ_*^r the magnitude of orientational order in the SN mixture is significantly larger than in the AN mixture due to the stiffer interface. However, the oscillatory structure exhibited by the needle profiles in the AN mixture is much more pronounced than in the SN case.

4.2. *The amphiphile distribution at the needle–sphere interface*

We next consider the question of how the amphiphiles are distributed at the free interface in a demixed SN mixture. In the following we restrict ourselves to low amphiphile chemical potentials, μ_A, such that the needle–sphere interface is only slightly modified by the presence of amphiphiles. We use μ_A as a control parameter to vary the number of amphiphilic particles entering the system. In the limit $\mu_A = -\infty$ we recover the binary SN mixture. The chemical potential is normalized through choice of the thermal wavelength Λ_A such that $\Lambda_A^3 = \pi\sigma_A^3/6$, and is expressed in units of thermal energy k_BT, where k_B is Boltzmann's constant and T is the temperature.

In order to fully understand the inhomogeneous ternary mixture it is first necessary to determine the location of the phase boundaries of the bulk system. To display the ternary phase diagrams in the most accessible way we first show the (η_s, ρ_*^r) plane for a fixed amphiphile chemical potential, μ_A. This allows clear identification of the coexisting sphere densities. Fig. 5a shows the (η_s, ρ_*^r) plane for four different values of amphiphile chemical potential $\mu_A = 0$, 15, 18, and 20. For values of $\mu_A \leqslant 10$ the phase boundary becomes indistinguishable from that of the SN mixture [35] on the scale of Fig. 5a. For $\mu_A = 15$ very few amphiphiles enter the system and the binodal is only slightly perturbed from the pure SN case. Increasing the amphiphile chemical potential to values $\mu_A > 15$ causes a dramatic change in the qualitative shape

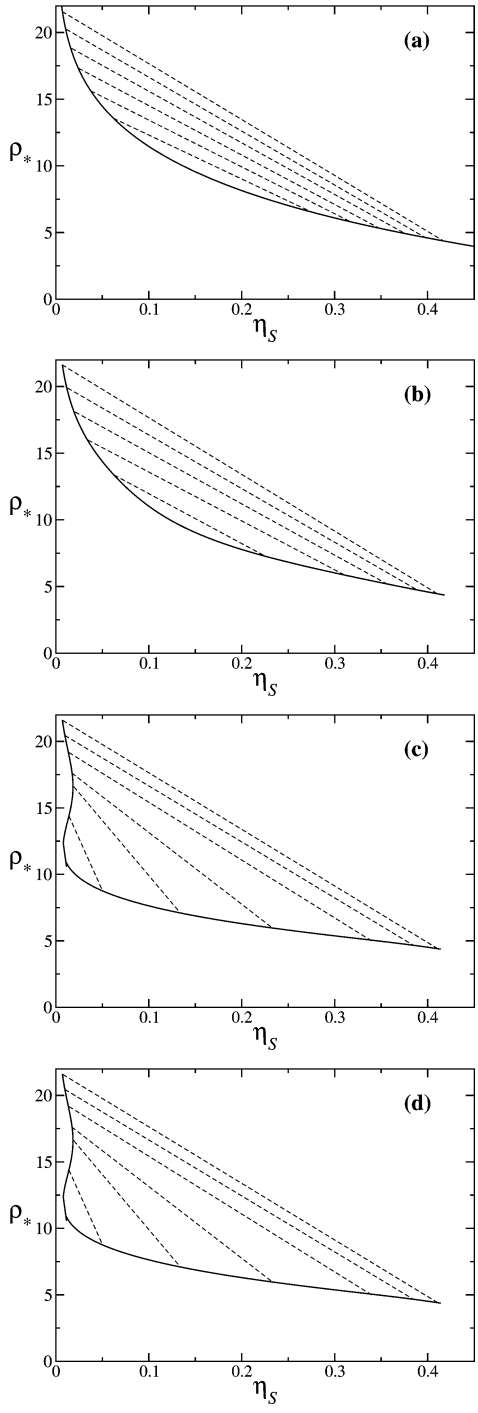

Fig. 6. The bulk phase diagram of the ternary ASN mixture in the (η_S, ρ_*) plane at four different values of the amphiphile chemical potential, μ_A. (a) $\mu_A = 0$, which, on the scale of the figure, is indistinguishable from the pure SN mixture for which $\mu_A = -\infty$, (b) $\mu_A = 15$, (c) $\mu_A = 18$, and (d) $\mu_A = 20$. As μ_A is further increased the critical point touches the vertical axis and then disappears. This signifies phase separation in the AN binary mixture.

of the binodal, with the critical point shifting to lower values of η_S. Fig. 5b shows the (η_A, ρ_*^r) plane and gives the coexisting amphiphile density in each phase. For reasons of clarity we omit the result for $\mu_A = 20$. In each case the larger of the two coexisting amphiphile densities corresponds to the sphere-rich phase, reflecting the fact that the hard-body amphiphiles prefer to mix with spheres than needles, at least for the size ratios considered here. Fig. 6 shows the same phase boundaries in the (η_S, ρ_*) plane which allows determination of the coexisting needle densities.

We next consider the distribution of amphiphiles at the interface of a demixed SN mixture. For the purpose of illustration we display results for the state point $\rho_*^r = 23$, $\mu_A = 18$, which is well away from the critical point and thus ensures a sizable difference in coexisting sphere densities. The value of $\mu_A = 18$ is sufficiently large to ensure that a reasonable number of amphiphiles can enter the system without modifying the bulk phase boundaries strongly.

Fig. 7a shows the sphere profile, Fig. 7b the angle-averaged needle density, and Fig. 7c the needle orientational order parameter. All three profiles lie close to those of the pure SN mixture being only weakly perturbed by the presence of amphiphiles. The needles order perpendicular to the interface on the needle-rich side and parallel on the sphere-rich side. While the parallel ordering is a rather trivial packing effect the perpendicular ordering is more interesting and reflects the tendency of the needles to poke through the gaps in the effective wall of spheres. The fact that our theoretical approach can capture the perpendicular order illustrates the level of sophistication of the fundamental measures method in accounting for subtle packing effects in hard-particle systems.

Fig. 7d shows the angle-averaged amphiphile density profile. The amphiphiles show a clear tendency to agglomerate at the SN interface with a peak in the amphiphile density which approaches twice the bulk value in the sphere-rich phase. By increasing ρ_*^r to values greater than the $\rho_*^r = 23$ considered here we find that the peak in amphiphile density at the interface becomes increasingly pronounced, relative to the bulk amphiphile densities. However, such states could be metastable with respect to possible crystalline phases.

Fig. 7e shows the orientational order parameter of amphiphiles. The strong positive peak in this quantity represents a key result of this work and clearly demonstrates that our model amphiphiles undergo ordering in the interfacial region which mimics that observed in real amphiphilic systems. The peak reaches a value of $\sim$0.25 indicating that this is a strong effect. Recall that a value of unity corresponds to a delta-distribution of amphiphile orientations at $\theta = 0$. Indeed, the orientational ordering of the amphiphiles is an order of magnitude larger than that of needles. The peak located at $z/\sigma \sim -0.4$ approximately corresponds to the Gibbs dividing surface of amphiphiles. Recall that we define our origin according to the Gibbs dividing surface of spheres. The orientational order parameter also presents a "shoulder" feature at $z/\sigma \sim 0.75$ which corresponds to the peak in the average density. In the absence of excess amphiphile adsorption at the interface the orientational order would decay into the bulk phases on either side of the dividing surface with similar decay lengths. However, the

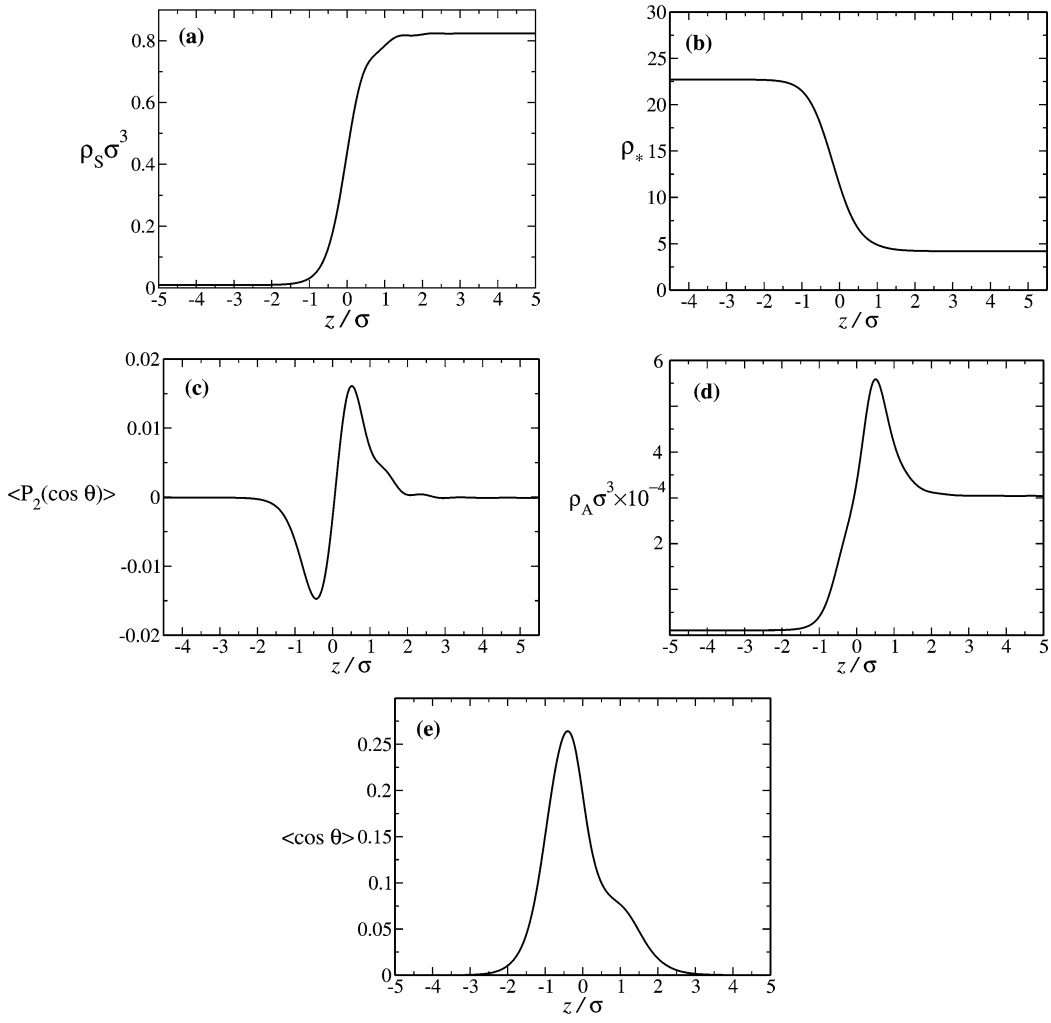

Fig. 7. Order parameter profiles of the ASN ternary mixture for $\rho_*^r = 23$ and $\mu_A = 18$. (a), (b), and (c) show the sphere density, the angle-averaged needle density, and the orientational order parameter, respectively, as a function of scaled distance along the z-axis. Due to the low amphiphile density in the system all three profiles lie close to those in the SN system. The angle-averaged amphiphile density profile, (d), exhibits a well-defined peak which reflects the agglomeration of amphiphiles at the interface. The positive value of the orientational order parameter of amphiphiles, (e), indicates that the amphiphiles collected at the interface have tails which point preferentially into the needle-rich phase.

agglomeration of amphiphiles on the sphere-rich side of the interface increases the penetration of parallel order into the sphere-rich phase. Preliminary results suggest that for larger values of ρ_*^r there is an increase in both the height of the peak in the orientational order parameter and the extent of the shoulder feature. It might be intuitively expected that larger ρ_*^r values would lead to a thinner layer of orientational ordering due to the increasing sharpness of the interface. However, the competition between the effects of increasing interfacial sharpness and increasing agglomeration of amphiphiles at the interface renders the thickness of the spatial orientation layer a nontrivial quantity.

5. Discussion

We have shown that a simple entropic model can successfully reproduce the phenomenology of amphiphilic particles at planar free interfaces. In the case of the demixed AN binary mixture the amphiphiles in the interfacial region tend to order perpendicular to the interface with tails which point preferentially into the needle-rich phase. In the ternary ASN mixture, when the density of amphiphiles is small, the amphiphiles agglomerate at the interface between sphere-rich and needle-rich phases, where they exhibit strong orientational ordering reminiscent of real amphiphilic systems. Although we consider an idealized model we believe that our qualitative findings are robust to perturbation and hope that our work will motivate future experimental studies of colloidal amphiphiles. The tunable nature of the interactions in colloidal systems, together with their experimental accessibility, has shed light on several fundamental aspects of liquid state physics which could not be addressed in atomic systems. By regarding colloids as model atoms one can take advantage of the increased length and time scales to investigate basic phenomena and test microscopic theories. Some exam-

ples of the success of this approach are the clarification of the role of attraction in the formation of stable liquid–vapor coexistence [15,16,25], increased understanding of the kinetics of crystallization [39] and, most recently, the successful verification of capillary wave theory by direct observation of thermally excited fluctuations of the free interface [40]. We suggest that similar insight into amphiphilic behavior may be gained from the study of colloidal amphiphilic systems.

The results presented here are very encouraging but it remains an open question as to whether our model amphiphiles are sufficient to stabilize higher level inhomogeneous structures. Perhaps the most likely structures to be formed by our model amphiphiles are spherical micelles. When a low concentration of amphiphile particles is added to a pure system of needles, a depletion attraction acts between the amphiphile heads, which leads to clustering. The orientational preference shown by the amphiphiles at the free AN interface, see Fig. 3, suggests that amphiphiles arriving at an existing cluster will tend to orient with tails pointing away from the center of mass, thus forming a micelle rather than an inverse micelle. The formation of such micelles and higher structures such as bilayer membranes or vesicles has been carried out for a phenomenological amphiphile model in [41] and it seems intuitive that similar effects could be presented by our microscopic model. Such an investigation would provide a natural extension of the present work.

Acknowledgment

The work of MS is part of the research program of the Stichting voor Fundamenteel Onderzoek der Materie (FOM), which is financially supported by the Nederlandse Organisatie voor Wetenschappelijk Onderzoek (NWO). Support by the DFG through the SFB TR6 is acknowledged.

References

[1] V.N. Manoharan, M.T. Elsesser, D.J. Pine, Science 301 (2003) 483.
[2] G.H. Koenderink, G.A. Vliegenthart, S.G.J.M. Kluijtmans, A. van Blaaderen, A.P. Philipse, H.N.W. Lekkerkerker, Langmuir 15 (1999) 4693.
[3] E.H.A. de Hoog, H.N.W. Lekkerkerker, J. Phys. Chem. B 103 (1999) 5274.
[4] E.H.A. de Hoog, H.N.W. Lekkerkerker, J. Schultz, G.H. Findenegg, J. Phys. Chem. B 103 (1999) 10,657.
[5] E.H.A. de Hoog, W.K. Kegel, A. van Blaaderen, H.N.W. Lekkerkerker, Phys. Rev. E 64 (2001) 021407.
[6] J.M. Brader, R. Evans, M. Schmidt, H. Löwen, J. Phys. Condens. Matter 14 (2002) L1.
[7] D.G.A.L. Aarts, J.H. van der Wiel, H.N.W. Lekkerkerker, J. Phys. Condens. Matter 15 (2003) S245.
[8] D.G.A.L. Aarts, H.N.W. Lekkerkerker, J. Phys. Condens. Matter 16 (2004) S4231.
[9] W.K. Wijting, N.A.M. Besseling, M.A. Cohen Stuart, Phys. Rev. Lett. 90 (2003) 196101.
[10] W.K. Wijting, N.A.M. Besseling, M.A. Cohen Stuart, J. Phys. Chem. B 107 (2003) 10,565.
[11] R. Roth, J.M. Brader, M. Schmidt, Europhys. Lett. 63 (2003) 549.
[12] S. Asakura, F. Oosawa, J. Chem. Phys. 22 (1954) 1255.
[13] S. Asakura, F. Oosawa, J. Polym. Sci. 33 (1958) 183.
[14] A. Vrij, Pure Appl. Chem. 48 (1976) 471.
[15] W.C.K. Poon, J. Phys. Condens. Matter 14 (2002) R859.
[16] R. Tuinier, J. Rieger, C.G. de Kruif, Adv. Colloid Interface Sci. 103 (2003) 1.
[17] J.M. Brader, R. Evans, Europhys. Lett. 49 (2000) 678.
[18] J.M. Brader, R. Evans, M. Schmidt, Mol. Phys. 101 (2003) 3349.
[19] M. Dijkstra, R. van Roij, Phys. Rev. Lett. 89 (2002) 208303.
[20] P.G. Bolhuis, D. Frenkel, J. Chem. Phys. 106 (1997) 666.
[21] G.A. Vliegenthart, Dissertation, Utrecht University, 1999.
[22] L. Helden, R. Roth, G.H. Koenderink, P. Leiderer, C. Bechinger, Phys. Rev. Lett. 90 (2003) 048301.
[23] K. Lin, J.C. Crocker, A.C. Zeri, A.G. Yodh, Phys. Rev. Lett. 87 (2001) 088301.
[24] G.A. Vliegenthart, H.N.W. Lekkerkerker, J. Chem. Phys. 111 (1999) 4153.
[25] H.N.W. Lekkerkerker, W.C.K. Poon, P.N. Pusey, A. Stroobants, P.B. Warren, Europhys. Lett. 20 (1992) 559.
[26] M. Schmidt, H. Löwen, J.M. Brader, R. Evans, Phys. Rev. Lett. 85 (2000) 1934.
[27] M. Schmidt, H. Löwen, J.M. Brader, R. Evans, J. Phys. Condens. Matter 14 (2002) 9353.
[28] M. Schmidt, Phys. Rev. E 63 (2001) 050201(R).
[29] P.G. Bolhuis, D. Frenkel, Physica A 244 (1997) 45.
[30] M. Schmidt, C. von Ferber, Phys. Rev. E 64 (2001) 051115.
[31] M. Schmidt, J. Phys. Condens. Matter 15 (2003) S101.
[32] P.G. Bolhuis, J.M. Brader, M. Schmidt, J. Phys. Condens. Matter 48 (2003) S3421.
[33] J.M. Brader, C. von Ferber, M. Schmidt, Mol. Phys. 101 (2003) 2225.
[34] L. Onsager, Ann. N.Y. Acad. Sci. 51 (1949) 627.
[35] J.M. Brader, A. Esztermann, M. Schmidt, Phys. Rev. E 66 (2002) 031401.
[36] R. Evans, Adv. Phys. 28 (1979) 143.
[37] Y. Rosenfeld, Phys. Rev. Lett. 63 (1989) 980.
[38] Y. Rosenfeld, M. Schmidt, H. Löwen, P. Tarazona, Phys. Rev. E 55 (1997) 4245.
[39] S. Auer, D. Frenkel, Phys. Rev. Lett. 91 (2003) 015703.
[40] D.G.A.L. Aarts, M. Schmidt, H.N.W. Lekkerkerker, Science 304 (2004) 847.
[41] A.M. Somoza, E. Chacón, L. Mederos, P. Tarazona, J. Phys. Condens. Matter 7 (1995) 5753.